

Enhancing cholesteric liquid crystal laser performance using a cholesteric reflector

Ying Zhou, Yuhua Huang, and Shin-Tson Wu

College of Optics and Photonics, University of Central Florida, Orlando, FL 32816

swu@creol.ucf.edu

<http://lcd.creol.ucf.edu>

Abstract: A high performance dye-doped cholesteric liquid crystal (CLC) laser is demonstrated by incorporating a passive CLC reflector to the active cell. The polarization-conserved CLC reflector effectively increases the distributed feedback cavity length which, in turn, results in a significant enhancement in lasing efficiency and a dramatic reduction in beam divergence. The lasing characteristics are still dominated by the circularly polarized light with the same sense as the cholesteric helix.

©2006 Optical Society of America

OCIS codes: (230.3720) Liquid-crystal devices, (160, 3710) Materials

References and links

1. V. I. Kopp, Z. Q. Zhang and A. Z. Genack, "Lasing in chiral photonic structures," *Prog. Quantum Electron.* **27**, 369-416 (2003).
2. S. T. Wu and D. K. Yang, *Reflective Liquid Crystal Displays*. (Wiley, New York, 2001)
3. J. P. Dowling, M. Scalora, M. J. Bloemer, and C. M. Bowden, "The photonic band edge laser: A new approach to gain enhancement," *J. Appl. Phys.* **75**, 1896-1899 (1994).
4. V. I. Kopp, B. Fan, H. K. M. Vithana, A. Z. Genack, "Low-threshold lasing at the edge of a photonic stop band in cholesteric liquid crystals," *Opt. Lett.* **23**, 1707-1709 (1998).
5. S. Y. Lin, J. G. Fleming, and I. Ei-Kady, "Experimental observation of photonic-crystal emission near a photonic band edge," *Appl. Phys. Lett.* **83**, 593-595 (2003).
6. M. Ozaki, M. Kasano, D. Ganzke, W. Haase, and K. Yoshina, "Mirrorless lasing in a dye-doped ferroelectric liquid crystal," *Adv. Mater.* **14**, 306-309 (2002).
7. W. Y. Cao, A. Munoz, P. Palffy-Muhoray, and B. Taheri, "Lasing in a three-dimensional photonic crystal of the liquid crystal blue phase," *Nat. Mater.* **1**, 111-113 (2002).
8. T. Matsui, R. Ozaki, K. Funamoto, M. Ozaki and K. Yoshino, "Flexible mirrorless laser based on a free-standing film of photo polymerized cholesteric liquid crystal," *Appl. Phys. Lett.* **81**, 3741-3743 (2002).
9. T. Ohta, M. H. Song, Y. Tsunoda, T. Nagata, K. C. Shin, F. Araoka, Y. Takanishi, K. Ishkawa, J. Watanabe, S. Nishimura, T. Toyooka, and H. Takezoe, "Monodomain film formation and lasing in dye-doped polymer cholesteric liquid crystal," *Jpn. J. Appl. Phys.* **43**, 6142-6144 (2004).
10. H. Finkelmann, S. T. Kim, A. Munoz, P. Palffy-Muhoray, and B. Taheri, "Tunable mirrorless lasing in cholesteric liquid crystalline elastomers," *Adv. Mater.* **13**, 1069-1072 (2001).
11. P. V. Hibaev, V. Opp, A. Enack, and E. Anelt, "Lasing from chiral photonic band gap materials based on cholesteric glasses," *Liq. Cryst.* **30**, 1391-1400 (2003).
12. Y. H. Huang, Y. Zhou, C. Doyle, and S. T. Wu, "Tuning the photonic band gap in cholesteric liquid crystals by temperature-dependent dopant solubility," *Opt. Express* **14**, 1236-1241 (2006).
13. S. Furumi, S. Yokoyama, A. Otomo, and S. Mashiko, "Electrical control of the structure and lasing in chiral photonic band-gap liquid crystals," *Appl. Phys. Lett.* **82**, 16-18 (2003).
14. M. F. Moreira, I. C. S. Carvalho, W. Cao, C. Bailey, B. Taheri, and P. Palffy-Muhoray, "Cholesteric liquid-crystal laser as an optic fiber-based temperature sensor," *Appl. Phys. Lett.* **85**, 2691-2693 (2004).
15. Y. Huang, Y. Zhou, and S. T. Wu, "Spatially tunable laser emission in dye-doped photonic liquid crystals," *Appl. Phys. Lett.* **88**, 011107 (2006).
16. A. Chanishvili, G. Chilaya, G. Petriashvili, R. Barberi, R. Bartolino, G. Cipparrone, and A. Mazzulla, L. Oriol, "Phototunable lasing in dye-doped cholesteric liquid crystals," *Appl. Phys. Lett.* **83**, 5353-5355 (2003).
17. A. Y. G. Fuh, T. H. Lin, J. H. Liu, and F. C. Wu, "Lasing in chiral photonic liquid crystals and associated frequency tuning," *Opt. Express* **12**, 1857-1863 (2004).
18. Y. Zhou, Y. Huang, A. Rapaport, M. Bass, and S. T. Wu, "Doubling the optical efficiency of a chiral liquid crystal laser using a reflector," *Appl. Phys. Lett.* **87**, 231107 (2005).

1. Introduction

Photonic band gap materials and devices which exhibit an ordered structure with periodic dielectric constant change have attracted much attention from both theoretical and practical viewpoints. With a photonic band gap, photons can be strongly localized within the band gap or at the band edge, which opens a way for achieving low-threshold lasers, micro-cavity lasers, optical diodes, and optical amplifiers [1].

With a self-organized chiral structure, cholesteric liquid crystal (CLC) is regarded as a promising one-dimensional (1D) photonic crystal. Although each CLC cell has a limited bandwidth, its fabrication method is much simpler than its 2D and 3D counterparts. In a cholesteric planar structure (Grandjean structure), the LC molecules are confined within the plane parallel to the substrates but rotated continuously from plane to plane with its helix perpendicular to the substrates. When a linearly polarized light passes through the CLC medium, it sees alternating ordinary and extraordinary refractive index (n_o and n_e) of the LC, giving rise to a polarization dependent reflection band due to Bragg reflection. If the incident light is circularly polarized and has the same sense as the cholesteric helix, then the light will be reflected, and the one in the counter handedness will be transmitted [2].

It has been theoretically predicted [3] that the electromagnetic modes are suppressed within the band gap but enhanced at the band edge because the group velocity tends to vanish near the band edge so that the density of states (DOS) and spontaneous emission rate are enhanced accordingly. The sharp increase of DOS at photonic band edge allows the possibility for generating a low threshold and high efficiency laser. Extensive work has been performed based on dye-doped CLC lasers where the cholesteric helical structure functions as a polarization-dependent distributed feedback (DFB) cavity for the active medium. The main advantages of a CLC laser are mirrorless, low threshold, and wide tuning range. So far, low threshold laser action has been demonstrated not only in chiral nematic liquid crystal [4, 5] but also in ferroelectric liquid crystal (Smectic C*) [6], blue phase liquid crystal [7], cholesteric polymer [8, 9], cholesteric elastomer [10] and more recently cholesteric glasses [11]. Tunability of lasing in these systems can be achieved by controlling the chiral agent concentration [12], external electric field [13], temperature [14, 15], mechanical stress [10], and photochemical effect [16, 17].

The central wavelength λ_o and bandwidth $\Delta\lambda$ of the CLC reflection band are determined by the following equations [2]:

$$\lambda_o = \langle n \rangle \cdot p, \quad (1)$$

$$\Delta\lambda = \Delta n \cdot p, \quad (2)$$

where $\langle n \rangle$ and Δn denote the average refractive index ($\langle n \rangle = (n_e + n_o)/2$) and birefringence ($\Delta n = n_e - n_o$) of the LC, and p is the intrinsic pitch length of the CLC employed. Here the intrinsic pitch length is defined as the distance along the helical axis over which the LC directors rotate by 2π , which is related to the helical twist power (*HTP*) of a chiral agent and the weight concentration $c\%$ as follows:

$$p = \frac{1}{HTP \cdot c\%} \quad (3)$$

Lasing efficiency and beam divergence are the two major concerns while designing a laser. They are mainly determined by two factors: the gain medium and the laser cavity structure. Higher lasing efficiency can be obtained by using an optical gain medium with higher emission efficiency. With the same optical gain medium, more efficient feedback from the

laser cavity is needed for obtaining higher laser efficiency. For a CLC laser, a thicker LC layer can provide a longer DFB and more efficient feedback which, in turn, increases the laser efficiency and reduces the beam divergence. However, the cell gap of a conventional CLC is usually limited to a few micrometers due to the weak anchoring force in the bulk area of a LC cell. As a result, the lasing efficiency of a CLC laser is highly restricted and such a short cavity length introduces highly divergent laser beam. Here, we focus our attention on the novel structure of laser cavity, capable of providing more efficient feedback for the emitted photons. Our previous work has successfully demonstrated that an additional CLC reflector on the active CLC lasing cell help boost the laser output power [18].

In this paper, we incorporate a passive CLC reflector to the dye-doped CLC active cell (master lasing cell) to serve as a polarization conserved reflector. Because of this CLC reflector, the effective laser cavity length is significantly increased. Consequently, the lasing efficiency is enhanced dramatically and the beam divergence is reduced significantly. Another advantage of this polarization conserved reflector is that it enables a higher lasing performance from a thinner active CLC layer. A thinner CLC cell is easier to obtain a defect-free morphology than a thicker layer due to stronger surface anchoring energy. To validate this hypothesis, we investigate the cell gap effects of the active CLC cell. An optimal cell gap for our dye-doped CLC laser system is about 10 μm . The corresponding physical mechanisms are explained.

2. Experiment

To fabricate an active CLC cell, we first prepared a right-handed CLC host mixture by mixing a Merck nematic liquid crystal BL006 ($n_e = 1.826$, $\Delta n = 0.286$ at $\lambda = 589$ nm and $T = 20$ °C) with 27.3% right-handed Merck chiral agent MLC-6248 ($\text{HTP} = 11.3 \mu\text{m}^{-1}$). Afterwards, we doped 1.5 wt% of a highly fluorescent Exciton DCM laser dye (4-(dicyanomethylene)-2-methyl-6-(4-dimethylaminoethyl)-4H-pran) to the CLC mixture. The whole mixture was thoroughly mixed before it was capillary-filled into the empty LC cell in an isotropic state. The inner surfaces of the glass substrates were first coated with a thin indium-tin-oxide (ITO) layer and then over coated with a thin (~80 nm) polyimide layer. The substrates were subsequently rubbed in anti-parallel directions to produce ~2-3° pretilt angle. A slow cooling process was necessary to obtain defect-free single domain morphology. To study the cell gap effects, we fabricated three active CLC cells with 8 μm , 10 μm , and 15 μm cell gaps. In a short pitch CLC layer, the strong chiral turn competes with the surface anchoring force so that multi-domain cholesteric defects cannot be completely eliminated, especially for the cell gap larger than 10 μm . Hence, light scattering is introduced which increases the loss in the laser cavity. To prepare a right-handed passive CLC reflector, we mixed ~25 wt% MLC-6248 into BL006. The passive CLC reflector has a 5 μm cell gap, whose reflection band covers the lasing wavelength of the active CLC laser. In the lasing experiment, the passive CLC cell is in proximity contact with the active CLC cell to avoid any air gap and interface reflections.

The morphologies of our three CLC active cells (8 μm , 10 μm , and 15 μm) and the 5 μm passive CLC reflector were investigated using a polarizing optical microscope (Objective 10X, Olympus). Results are shown in Figs. 1(a)-1(d), respectively. As the cell gap increases from 5 μm to 15 μm , the single domain of cholesteric planar structure gradually deteriorates and defect lines begin to aggregate, which results in a higher scattering loss in a thicker cell, e.g., the 15 μm cell.

The color difference in Fig. 1(d) originates from the different chiral concentration of the passive CLC reflector. From Eq. (3), a larger chiral concentration leads to a shorter pitch length and hence a shorter reflection wavelength (green).

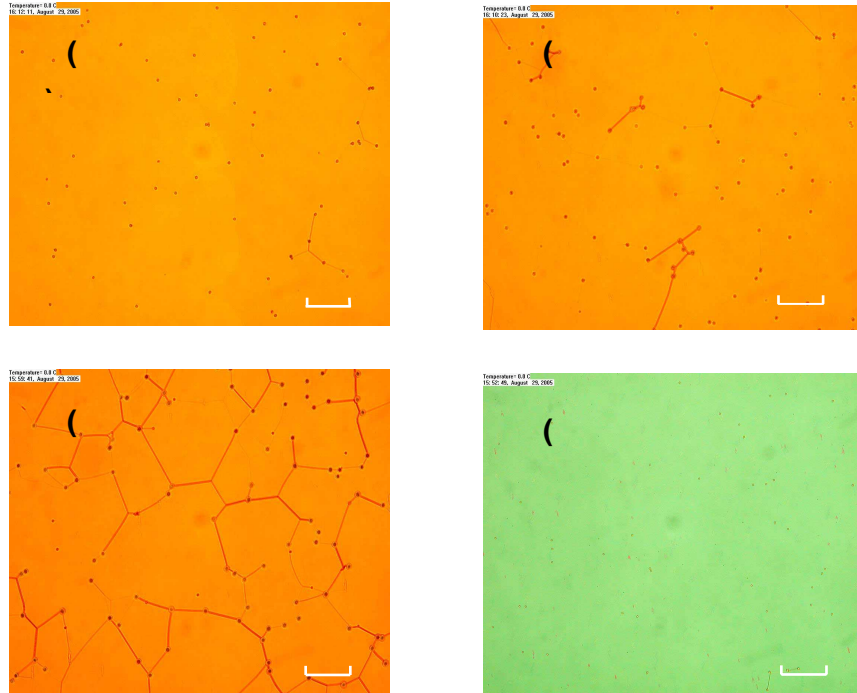


Fig. 1. Microscopy images of cholesteric liquid crystal morphologies: (a) 8 μm DCM-doped CLC cell, (b) 10 μm DCM-doped CLC cell, (c) 15 μm DCM-doped CLC cell, and (d) 5 μm CLC cell. The white bar in each figure shows a scale of 100 μm .

Figure 2 sketches the experimental setup for characterizing the CLC laser efficiency and beam divergence. The pumping source is a frequency-doubled Nd:YAG pulsed laser (Minilite II, Continuum) with wavelength $\lambda=532$ nm, 4 ns pulse width, and 1 Hz repetition rate. The reason we chose such a low repetition rate is to reduce the thermal accumulation inside the active CLC cell. The local temperature increase at pumping area is estimated to be $\sim 10^\circ\text{C}$, which does not affect the local cholesteric planar structure too noticeably because the mixture's clearing point is above 100°C . The pumping beam was separated into two channels by a beam splitter: one was sent to an energy meter (Laserstar, Ophir) for monitoring the input energy and the other was focused onto the CLC cell. Because the absorption dichroism of the dye molecules is distributed in a helical manner, the CLC laser does not exhibit any polarization preference for the pumping beam [19]. However, we chose the left-handed circularly polarized (LCP) light to pump the right-handed CLC cell in order to reduce Bragg reflection even if the reflection band overlaps with the pumping wavelength. Since the reflection band of the passive CLC layer covers the lasing wavelength but transmits the pumping wavelength, the configuration in normal incident pump will reduce the surface reflection to its maximum. The emitted laser light is collected into a fiber-based spectrometer (Ocean Optics, HR2000, resolution=0.4 nm) along the direction exactly perpendicular to the glass substrates where lies the periodic refractive index modulation.

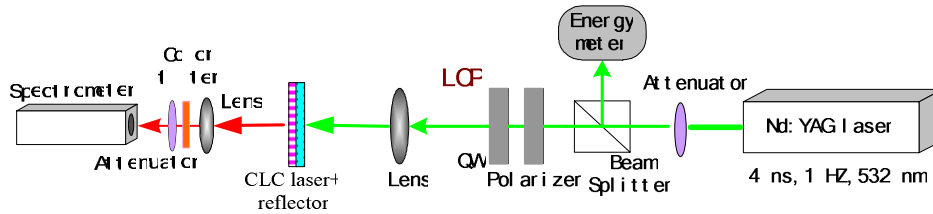


Fig. 2. Experimental setup; LCP: Left-handed circularly polarized light, and QW: Quarter wave plate.

3. Experimental results and discussions

3.1 CLC laser output power

Figure 3 shows the wavelength dependent normalized transmittance of the three active CLC cells at 8 μm , 10 μm , and 15 μm gaps and the passive CLC cell at 5 μm gap. The lasing spectrum using a single 8 μm active CLC cell pumped at 30 $\mu\text{J}/\text{pulse}$ is also included in the figure as an example. It is seen that the reflection band of the passive cell covers the photonic band edge (long wavelength edge) of the active cell where lasing takes place. The short wavelength edges of the active CLC cells are obscured by the DCM absorption. The full width of half maximum (FWHM) of the lasing spectrum was measured to be 0.8–1.0 nm. The lasing wavelength for the single 8 μm , 10 μm , and 15 μm cell is located at around $\lambda=603\text{ nm}$.

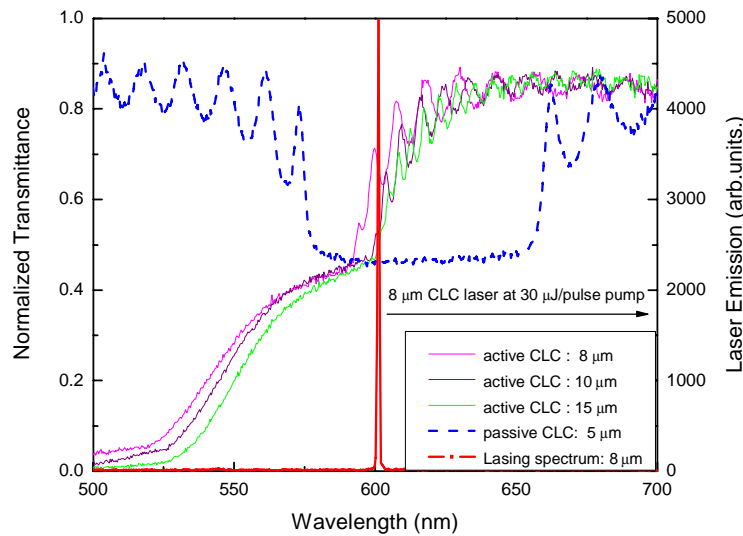


Fig. 3. Wavelength dependent normalized transmittance of three active CLC cells (8, 10, and 15 μm) and a passive CLC cell (5 μm). The red line is the lasing spectrum of the 8 μm active CLC cell at 30 $\mu\text{J}/\text{pulse}$ pump.

To demonstrate how the CLC reflector improves the lasing efficiency and reduces beam divergence, we have conducted experiments using an active CLC cell with/without the CLC reflector. Figures 4-6 plot the pumping energy dependent lasing performance using a 5 μm passive CLC cell combined with the 8, 10, and 15 μm active cells respectively and compare the performance to those without the passive CLC cell. The passive CLC reflector is kept at 5 μm for two reasons: 1) it provides enough reflectivity at the lasing wavelength, and 2) the thin layer is defect-free. In Figs. 4-6, the red and magenta curves represent the total laser output

power and its corresponding left-handed circularly polarized (LCP) component for the active-passive layered CLC laser, respectively. Similarly, blue and green curves are for the single layer CLC lasers. The lasing threshold for the single 8, 10, and 15 μm active cells was measured to be 1.8, 1.0, and 0.5 $\mu\text{J}/\text{pulse}$, respectively. Laser action was observed at the long wavelength band-edge but at a slightly different wavelength (603, 604, and 604 nm). With the passive CLC reflector, the lasing threshold does not drop noticeably because the laser output intensity is unstable near the threshold. As a result, the threshold change could be easily obscured by the intensity fluctuation of the pumping pulse. A remarkable threshold drop (from 22 to 10 $\mu\text{J}/\text{pulse}$) was observed when using a 5 μm -thick active cell and the same passive reflector. However, the 5- μm CLC double-cell assembly has a much lower lasing efficiency so that its data are not included here for comparison. The fluctuations observed in the curves result from the fluctuation of the pumping Nd-YAG laser and different reflection point on the passive cell each time a pulse is captured.

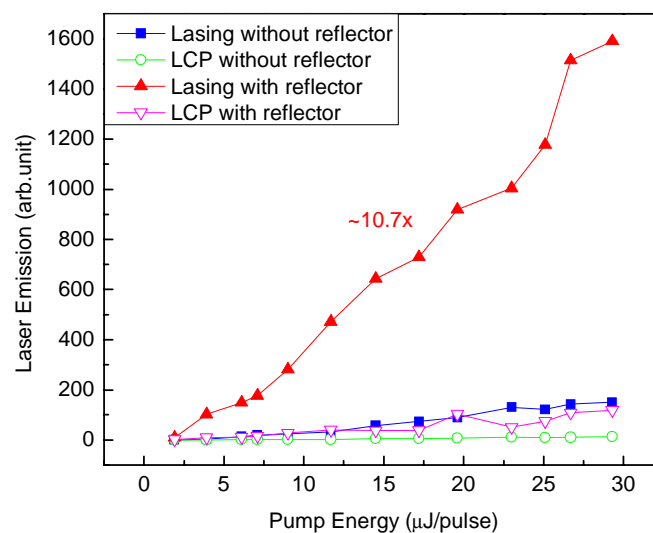


Fig. 4. Pumping energy dependent laser output power of the 8- μm active CLC cell with a 5 μm passive CLC reflector. Threshold ~ 1.8 $\mu\text{J}/\text{pulse}$ at $\lambda=532$ nm. The average enhancement ratio is $\sim 10.7X$.

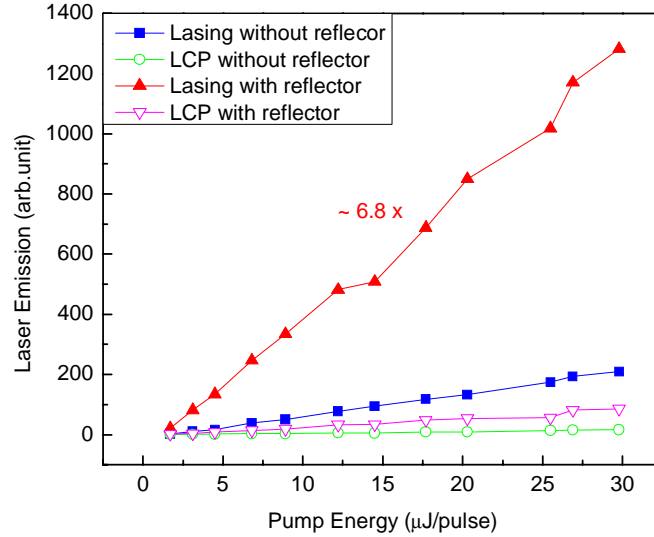


Fig. 5. Pumping energy dependent laser output power of the 10- μm active CLC cell with a 5 μm passive CLC reflector. Threshold ~ 1.0 $\mu\text{J}/\text{pulse}$ at $\lambda=532$ nm. The average enhancement ratio is $\sim 6.8\text{X}$.

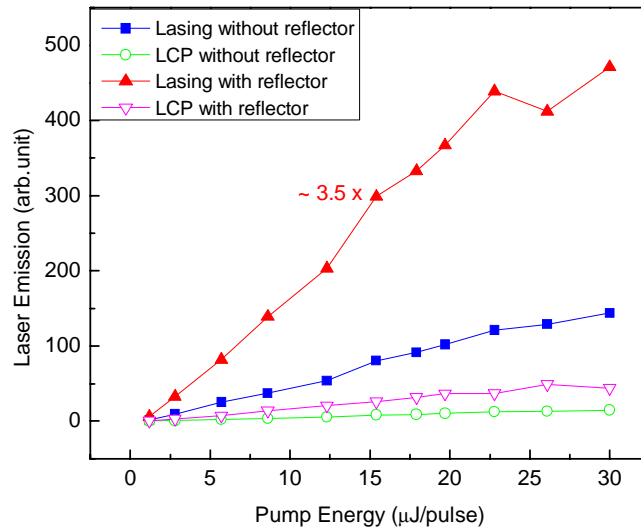


Fig. 6. Pumping energy dependent laser output power of the 15- μm active CLC cell with a 5 μm passive CLC reflector. Threshold ~ 0.5 $\mu\text{J}/\text{pulse}$ at $\lambda=532$ nm. The average enhancement ratio is $\sim 3.5\text{X}$.

From Figs. 4-6, the single active CLC laser generates a circularly polarized light in the same handedness as the cholesteric helix (right-handed circularly polarized (RCP) light in our case). As a consequence of CLC-based polarization selective DFB, only circularly polarized

light in the same handedness experiences high reflectivity inside the cavity. Yet a small part (<10%) of the opposite circularly polarized light (LCP) exists due to the imperfection of CLC's periodic structure and the surface reflection from the glass substrates.

In a double-cell CLC structure, laser output power is enhanced by more than twice (actually 3.5–10.7X) in all the three lasers studied despite of their different active layer thickness. Besides, RCP component still dominates the total output. That means the reflected light from the CLC reflector gets further amplified by the gain medium. In the same helical handedness as the master CLC lasing cell, the passive CLC reflector well preserves the original polarization state of the reflected beam without introducing π phase change. As a result, the reflected beam is still at band edge wavelength and more importantly, in the same polarization state as can be facilitated by DFB cavity for a band edge mode resonance. Under this circumstance the passive cell functions equivalently as a “polarization conserved reflector” for the polarization selective cavity and the effective length of the amplifier is therefore doubled.

However, the lasing enhancement ratio due to the passive CLC reflector is different for the three lasing samples. Figures 4-6 show that the enhancement ratio decreases as the master CLC cell gap increases. Usually, a thicker CLC cell provides a longer DFB length, i.e., a larger optical gain which leads to a higher lasing efficiency. Nevertheless another two factors contributes to the enhancement as well: 1) the increase of net gain (the difference between gain and loss in the cavity) due to passive CLC reflector, and 2) how much light can be reflected back into the original cavity. With a virtually length-doubled amplifier and feedback, both gain and loss are simultaneously doubled. One can benefit from a doubled net gain caused by a length doubled amplifier if the single path net gain is positive. As long as the total length is below the saturation length (the length corresponding to the saturation output intensity), the output power grows exponentially with the increase of gain length, leading to the dramatic enhancement we observed. On the other hand, the overlap of the original laser beam and the reflected laser beam creates the possibility of further amplification. For a single layer CLC laser, a thicker cell has smaller beam divergence but also a smaller acceptance angle for the reflected beam. Because the passive “polarization conserved CLC mirror” is not curved, it further diverges the beam upon reflection. Thus the smaller acceptance angle in a thicker cell restricts the output enhancement more heavily. According to our experimental results, the acceptance angle is the killing factor which determines the enhancement ratio.

In addition to the dramatic enhancement of the output laser power, the polarization conserved CLC reflector also reduces the beam divergence significantly. Details are discussed in the following section.

3.2. CLC laser beam divergence and beam profile

Using a high speed CCD camera (ST-2000XM, SBIG), we captured the CLC laser beam spot at a gradually increased distance from the lasing cell. For comparison, the far field patterns of the CLC lasers with and without a passive CLC reflector for the 8 μm , 10 μm , and 15 μm active cells were measured. Results are compared in Figs. 7-9.

From Figs. 7-9, we find that as the observation plane moving further away the beam spot size increases quickly. Here, we mainly refer to the center spot since the outer fringes are caused by diffraction. For the single layer active CLC laser, half divergence angle was measured to be 4.43°, 4.65°, and 4.77° for the 8, 10, and 15 μm cell gaps, respectively. A thinner cell seems to have a slightly less divergence than a thicker cell but the difference is quite insignificant considering the measurement error. The large divergence angle of CLC laser originates from the short gain medium length (in μm scale) and the small cross-section area of the emission (~150 μm in diameter). Usually the longer cavity length the smaller divergence angle it is. The reason why the 15 μm laser does not show an obvious advantage in beam divergence is owing to the strong light scattering from the defect lines.

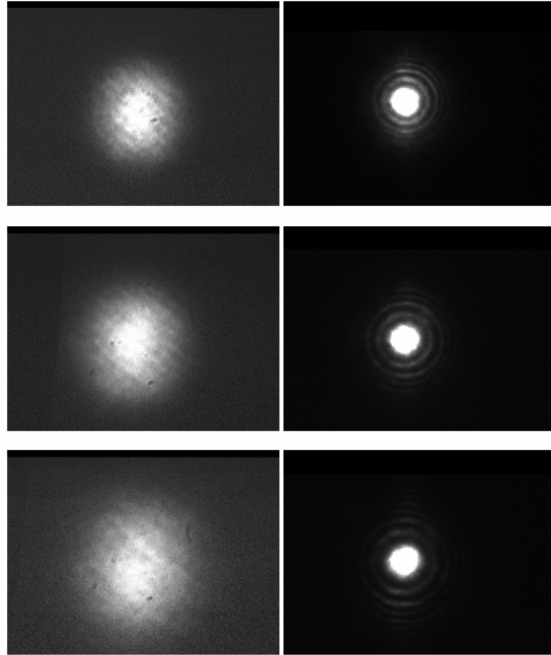


Fig. 7. Far field laser patterns of the 8- μm CLC laser at 3.2 cm (top), 4.3 cm (middle), 5.3 cm (bottom) away from the lasing cell. Pumping laser energy is 38 $\mu\text{J}/\text{pulse}$ and $\lambda = 532$ nm. Left column: single active layer CLC lasers; Right column: active-passive layered CLC lasers.

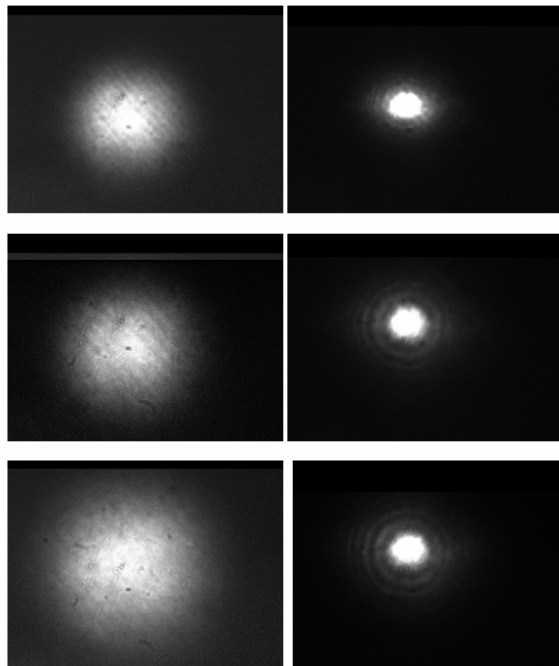


Fig. 8. Far field laser patterns of the 10- μm CLC laser at 3 cm (top), 4 cm (middle), and 5 cm (bottom) away from the lasing cell. Pumping laser energy is 38 $\mu\text{J}/\text{pulse}$ and $\lambda = 532$ nm. Left column: single active layer CLC lasers; Right column: active-passive layered CLC lasers.

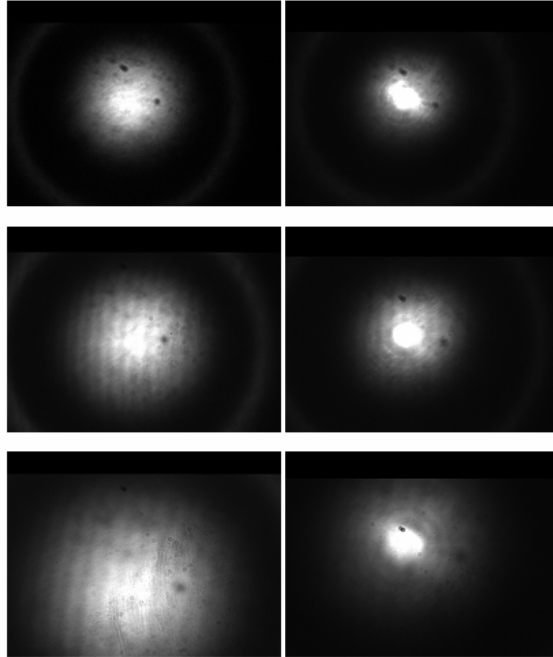


Fig. 9. Far field laser beam spot of 15- μm CLC laser at 2.5 cm (top), 3.3 cm (middle), 5.0 cm (bottom) away from lasing cell. Pumping laser energy is 38 $\mu\text{J}/\text{pulse}$ and $\lambda = 532$ nm. Left column: single active layer CLC lasers; Right column: active-passive layered CLC lasers.

By incorporating a passive CLC reflector to the master lasing cell, the laser spot dramatically shrinks with clearer diffraction fringes. Laser emission energy also becomes much more concentrated within the central spot and the peak intensity remarkably increases. The half divergence angles for the active-passive layered CLC lasers decrease to 0.69° , 0.69° , and 0.37° for the 8, 10, and 15 μm cell gaps, respectively, considering the bright center spot only. No distinct increase in spot size is observed except the appearance of a halation circle around the central spot for the 15 μm double-layered laser whose divergence angle is $\sim 3^\circ$.

This evident improvement of beam divergence from the active/passive CLC lasers is due to the effectively increased cavity length. By adding a passive CLC cell which is a “plane mirror”, we introduce two glass substrates (totally 2.2 mm thick) of the LC cells into the cavity so that the cavity length, as a whole, is increased from μm scale to mm scale. Though a virtually doubled gain length also contributes to the decrease of divergence angle, the insert of glass substrate plays a dominant role. In the 15- μm double-layered laser, multi-domain scattering not only limits the output power but also causes degradation of long-range periodic structure within the cell gap. This is why we observed the extra halation around the main spot.

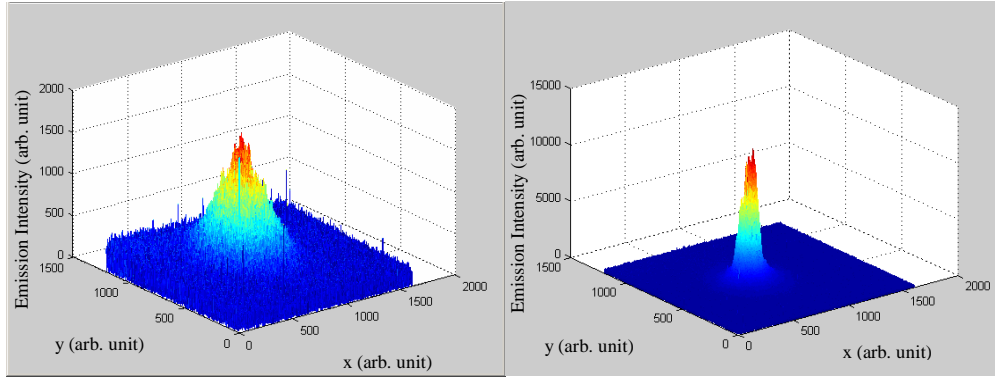


Fig. 10. Comparison of the far field 2D beam profiles from the 10- μm single layer CLC laser (left) and the 10- μm double-layered CLC laser (right). The images are extracted from Fig. 8 at distance 3 cm away. Pumping energy is 38 $\mu\text{J}/\text{pulse}$, $\lambda=532$ nm.

As an example, we extracted the beam profile from the CCD pictures shown in the middle row of Fig. 8. Figure 10 shows the 2D beam profile of the 10- μm single layer CLC laser (left) versus 10- μm double-layered CLC laser (right) at 3 cm away and 38 $\mu\text{J}/\text{pulse}$ pumping energy. The beam shape is neither Gaussian nor Lorentzian, which implies higher order transverse modes should be present, leading to the increased divergence.

4. Conclusions

We have demonstrated a photonic band edge lasing from the double cell CLC structure comprising of an active CLC cell and a polarization-conserved CLC reflector. Compared to the single cell CLC laser, the double cell structure shows dramatic improvement in both laser output power and beam divergence. With the reflection band covering the lasing wavelength, the passive CLC reflector works as a polarization-conserved reflector so that the length of the amplifier is equivalently doubled and the total cavity length is increased by 100 times. Based on this work, the optimal output from a CLC laser is achieved in the active CLC cell where single domain morphology is maintained.